Supplemental material to this article can be found at:
http://dmd.aspetjournals.org/content/suppl/2021/05/05/dmd.120.000322.DC1

1521-009X/49/7/509–520$35.00
DRUG METABOLISM AND DISPOSITION

https://doi.org/10.1124/dmd.120.000322
Drug Metab Dispos 49:509–520, July 2021

Development and Verification of a Linked Δ^9-THC/11-OH-THC Physiologically Based Pharmacokinetic Model in Healthy, Nonpregnant Population and Extrapolation to Pregnant Women[S]

Gabriela I. Patilea-Vrana[1] and Jashvant D. Unadkat

Department of Pharmaceutics, University of Washington, Seattle, Washington

Received November 27, 2020; accepted April 6, 2021

ABSTRACT

Conducting clinical trials to understand the exposure risk/benefit relationship of cannabis use is not always feasible. Alternatively, physiologically based pharmacokinetic (PBPK) models can be used to predict exposure of the psychoactive cannabinoid (−)-Δ^9-tetrahydrocannabinol (THC) and its active metabolite 11-hydroxy-Δ^9-tetrahydrocannabinol (11-OH-THC). Here, we first extrapolated in vitro mechanistic pharmacokinetic information previously quantified to build a linked THC/11-OH-THC PBPK model and verified the model with observed data after intravenous and inhalation administration of THC in a healthy, nonpregnant population. The in vitro to in vivo extrapolation of both THC and 11-OH-THC disposition was successful. The inhalation bioavailability (F_{inh}) of THC after inhalation was higher in chronic versus casual cannabis users (F_{inh} = 0.35 and 0.19, respectively). Sensitivity analysis demonstrated that 11-OH-THC but not THC exposure was sensitive to alterations in hepatic intrinsic clearance of the respective compound. Next, we extrapolated the linked THC/11-OH-THC PBPK model to pregnant women. Simulations showed that THC plasma area under the curve (AUC) does not change during pregnancy, but 11-OH-THC plasma AUC decreases by up to 41%. Using a maternal-fetal PBPK model, maternal and fetal THC serum concentrations were simulated and compared with the observed THC serum concentrations in pregnant women at term. To recapitulate the observed THC fetal serum concentrations, active placental efflux of THC needed to be invoked. In conclusion, we built and verified a linked THC/11-OH-THC PBPK model in healthy nonpregnant population and demonstrated how this mechanistic physiologic and pharmacokinetic platform can be extrapolated to a special population, such as pregnant women.

SIGNIFICANCE STATEMENT

Although the pharmacokinetics of cannabinoids have been extensively studied clinically, limited mechanistic pharmacokinetic models exist. Here, we developed and verified a physiologically based pharmacokinetic (PBPK) model for (−)-Δ^9-tetrahydrocannabinol (THC) and its active metabolite, 11-hydroxy-Δ^9-tetrahydrocannabinol (11-OH-THC). The PBPK model was verified in healthy, nonpregnant population after intravenous and inhalation administration of THC, and then extrapolated to pregnant women. The THC/11-OH-THC PBPK model can be used to predict exposure in special populations, predict drug-drug interactions, or impact of genetic polymorphism.

Introduction

As of November 2020, 36 states in the United States allow either medical (21 states) and/or recreational (15 states) use of marijuana (cannabis) (https://www.ncsl.org/research/health/state-medical-marijuana-laws.aspx). In 2018, an estimated 40.3 million adults, which corresponds to 15.9% of the population in the United States, used cannabis (SAMHSA, 2018). Concentrations of (−)-Δ^9-tetrahydrocannabinol (THC), the psychoactive constituent of cannabis, have been increasing, with estimated mean THC concentrations of 17.1% (Chandra et al., 2019). THC is eliminated from the body primarily by hepatic cytochrome P450 enzyme 2C9 metabolism, and this pathway also results in the production of its main psychoactive metabolite, 11-hydroxy-Δ^9-tetrahydrocannabinol (11-OH-THC) (Patilea-Vrana and Unadkat, 2019). 11-OH-THC is cleared from the body by CYP3A, CYP2C9, and UGT metabolism (Patilea-Vrana and Unadkat, 2019).

Cannabis is consumed by a spectrum of individuals spanning from those taking Food and Drug Administration-approved drugs or supplements, pregnant women, to those with hepatic or renal impairment.

This work was supported by the National Institutes of Health National Institute on Drug Abuse [Grant P01-DA032507] (to G.P-V. and J.D.U.) and the Rene Levy Fellowship to G.P-V.

The authors report no conflicts of interest.

[1]Current affiliation: Seagen, Inc., Bothell, Washington.

This manuscript constituted part of G.P-V.'s dissertation: Patilea-Vrana GI (2019) Predicting Maternal-Fetal Cannabinoid Exposure During Pregnancy Using Physiologically-Based Pharmacokinetic Modeling and Simulation. Doctoral dissertation, University of Washington, Seattle, WA.

[S] This article has supplemental material available at dmd.aspetjournals.org.

ABBREVIATIONS: AUC, area under the curve; $AUC_{0\text{-}t}$, area under the curve from 0 to time t; AUCR, AUC ratio; BCRP, breast cancer resistance protein; CL, clearance; CL_{int}, intrinsic clearance; COOH-THC, 11-nor-9-caroboxy-Δ^9-THC; F_{inh}, inhalation bioavailability; F/M, fetal to maternal; fm, fraction metabolized; ft, fraction transported; fu_{inc}, fraction unbound in human liver microsome incubation; fu_p, fraction unbound in plasma; GC-MS, gas chromatograph–mass spectrometry; GW, gestational week; Kp, tissue:plasma partition coefficient; m-f-PBPK, maternal-fetal PBPK; M/P, metabolite to parent ratio; mPBPK, minimal PBPK; MRE, mean relative error; M&S, modeling and simulation; NLME, nonlinear mixed effects; 11-OH-THC, 11-hydroxy-Δ^9-tetrahydrocannabinol; PBPK, physiologically based pharmacokinetic modeling; P-gp, P-glycoprotein; PK, pharmacokinetics; rRMSE, relative root mean square error; RSE, relative S.E.; T1, first trimester; T2, second trimester; T3, third trimester; THC, (−)-Δ^9-tetrahydrocannabinol; TLC, thin-layer chromatography; UGT, UDP-glucuronosyltransferase; V_{ss}, volume of distribution at steady state.

Therefore, it is possible that the disposition of THC/11-OH-THC in special populations (e.g., pregnant women or patients with hepatic impairment) may be altered, or THC/11-OH-THC exposure may be impacted by drug-drug interactions. The impact of altered THC/11-OH-THC disposition on safety and efficacy under the aforementioned scenarios needs to be further studied. However, conducting studies, especially in pregnant women, to address these questions is ethically and logistically challenging. One approach to overcoming this dilemma is to first develop a physiologically based pharmacokinetic model (PBPK) of THC/11-OH-THC disposition using the bottom-up approach. Then, this PBPK model can be interrogated as to how changes in physiology in special populations or drug interactions will impact the disposition of THC/11-OH-THC. As such, the aims of this study were 1) to build a linked THC/11-OH-THC PBPK model using a bottom-up approach by extrapolating previously quantified in vitro enzyme kinetics of THC and 11-OH-THC (Patilea-Vrana et al., 2018), 2) to verify the THC/11-OH-THC PBPK model after intravenous and inhalation administration of THC in a healthy nonpregnant population, and finally 3) to extrapolate the verified THC/11-OH-THC PBPK model in healthy nonpregnant population to pregnant women and predict maternal and fetal cannabinoid serum concentrations. The final THC and 11-OH-THC PBPK models were verified after intravenous and inhalation but not oral administration of THC, since mechanistic data on extrahepatic metabolism is missing. Importantly, smoking cannabis is the most popular and therefore relevant route of administration (Schauer et al., 2016).

We chose to extrapolate the THC/11-OH-THC PBPK model to pregnant women since pregnant women are a special population often not studied. There are also concerns surrounding fetal exposure to THC/11-OH-THC. Epidemiologic studies have shown that maternal cannabis use leads to poorer neonatal outcomes (Grzeskowiak et al., 2020) and subtle but persistent neurodevelopmental consequences (Stickrath, 2019). Prospective clinical studies to quantify the risk of maternal cannabis use are not ethical. Alternatively, if the maternal and fetal THC and 11-OH-THC exposure during pregnancy is known, then the risk associated with maternal cannabis use can be anticipated. Measuring maternal and fetal drug exposure clinically is not ethical. Therefore, the only safe alternative to predict THC/11-OH-THC exposure during pregnancy is via PBPK modeling and simulation (M&S). This can be achieved by extrapolating the THC/11-OH-THC PBPK model verified in healthy, nonpregnant population to pregnant women by accounting for gestational age physiologic changes, such as changes to the activity of drug metabolizing enzymes and expression of drug binding proteins. Our laboratory has previously demonstrated the validity of using PBPK M&S to successfully predict maternal and fetal exposure of a variety of drugs (Ke et al., 2012, 2014; Zhang and Unadkat, 2017).

Materials and Methods

Meta-analysis of THC and 11-OH-THC Exposure after Intravenous and Inhalation of Either THC or 11-OH-THC to Identify Optimal Datasets for PBPK Model Training and Verification. The inclusion criteria for clinical studies used for PBPK model development included single dose studies in healthy nonpregnant subjects where THC and 11-OH-THC were administered either intravenous or via inhalation with no exclusions made for sample size, gender, frequency of cannabis use, or bioanalytical methodology. Where available, plasma/serum or blood concentration-time profiles were digitized using the online semiautomatic tool WebPlotDigitizer (https://automeris.io/WebPlotDigitizer/). If not reported, the plasma/serum or blood area under the concentration-time curve (AUC) was estimated via noncompartmental analysis using Phoenix 8.1, Certara (Princeton, NJ). The details and observed PK parameters after intravenous administration of THC or 11-OH-THC and after inhalation of THC can be found in Supplemental Tables 1 and 2, respectively. Unless otherwise specified, plasma/serum concentrations and PK parameters are reported. Throughout this entire manuscript, observed or simulated plasma concentrations are assumed to be similar to serum concentrations.

To assess the quality of the observed data and identify any potential outliers, the observed THC and 11-OH-THC concentration-time profiles were dose normalized (Supplemental Fig. 1). As shown in Supplemental Fig. 1A, studies that used thin-layer chromatography (TLC) had remarkably different plasma concentration-time profiles compared with all other studies, particularly at timepoints > 12 hours postdose. For example, THC plasma clearance (CL) estimated via TLC (Wall et al., 1983) was 12–15 l/h, whereas studies that used high performance liquid chromatography-UV (Hunt and Jones, 1980) or gas chromatograph–mass spectrometry (GC-MS) (Ohlsson et al., 1982; Kelly and Jones, 1992; Naef et al., 2004) estimated THC plasma clearance between 36 and 59 l/h. Similarly, a much longer terminal half-life was observed in the TLC studies (Lemberger et al., 1970; Lemberger et al., 1971, 1972b; Wall et al., 1983) when compared with the remaining studies (Supplemental Table 1). It should be noted that the TLC studies are from two different groups, so it is likely that the analytical methodology of TLC versus high performance liquid chromatography-UV or GC-MS contributed to the difference. Furthermore, it has been noted that less selective methodologies, such as TLC, are unable to distinguish THC isomers (Wall et al., 1972). This may be a potential reason for the higher Δ^9-THC concentrations measured at later timepoints via TLC when compared with other methodologies. Since characterization of the terminal phase kinetics was crucial during model development, all TLC studies were removed and not used during THC or 11-OH-THC PBPK model training and verification. Lastly, the study from Brenneisen et al., 2010 was removed from the THC inhalation datasets since both THC and 11-OH-THC plasma concentrations were at least one order of magnitude smaller than all other studies. The reason for this discrepancy is unknown.

Details of the studies used for PBPK model training and development are shown in Table 1. All the studies had small sample sizes (n = 3–22), had mostly male subjects, and were of younger age. There is large interindividual as well as interstudy variability (see Supplemental Tables 1 and 2 for further details). A designation of naïve, casual, or chronic cannabis users was given for no previous cannabis use, cannabis use less than twice a week, and cannabis use greater than twice a week, respectively. The designation for chronic or casual cannabis use was chosen arbitrarily but guided by the general categorization of cannabis use frequency in the studies shown in Table 1.

Estimation of Population THC Volume of Distribution at Steady State and Inhalation Absorption Kinetics via Nonlinear Mixed Effects Modeling. Due to its high lipophilicity, THC volume of distribution at steady state (V_{ss}) was severely overestimated in the initial PBPK model. Hence, the THC PBPK model–predicted V_{ss} needed to be fixed to the observed THC V_{ss}. As shown in Supplemental Table 1, the reported THC V_{ss} ranged from 0.6–8.9 l/kg (Hunt and Jones, 1980; Kelly and Jones, 1992; Naef et al., 2004). However, the smaller V_{ss} values are likely underestimates of the true V_{ss} because of shorter total blood sampling times (e.g., 8 versus 24 hours). Additionally, there is no mechanistic information on lung disposition of THC in humans. Because of these limitations, the observed THC V_{ss} as well as the absorption rate constant (ka) and bioavailability (F_{inh}) after inhalation of THC were estimated by simultaneously fitting a three-compartment model without and with absorption compartment to the digitized plasma/serum concentration-time profiles after intravenous and inhalation administration of THC, respectively, using a nonlinear mixed effects (NLME) model in Phoenix 8.1, Certara (Princeton, NJ) (Supplemental Fig. 2). In using this approach, we assumed that the mean data set from each study constituted an individual subject. We recognize that this is not usual for NLME analyses of data, but our approach suffices for our goal, that is to obtain mean population parameters for THC V_{ss}, F_{inh}, and ka to use in our PBPK model.

THC PBPK Model Development and Verification in Healthy Nonpregnant Population. The linked THC/11-OH-THC PBPK model development in a healthy nonpregnant population using Simcyp (Simcyp population-based simulator version 16, Simcyp Limited, Sheffield, UK) is outlined in Fig. 1. Final input values for the THC PBPK model are listed in Table 2. Physicochemical properties for THC were collected from literature. We have previously measured the in vitro kinetics (V_{max} and K_m) of THC via CYP2C9 [major pathway, fraction metabolized (fm) = 0.91] and CYP2D6 (fm = 0.09) (Patilea-Vrana and Unadkat, 2019). These values, which are listed in Table 2, were extrapolated to in vivo using enzyme expression levels as listed in the Simcyp Virtual Healthy Population. Renal and biliary clearance were set to 0 l/h, since less than 5% of administered THC dose is excreted unchanged in urine and feces (Wall and Perez-

TABLE 1

Datasets used for THC and 11-OH-THC PBPK model training and verification

Study Name	Administration	THC Dose	Sampling Time	N (Subjects)	Females (%)	Age	Average Frequency of Cannabis Use	Cannabis User[c]	Reference
			hr						
Hunt_1980	Intravenous	2 mg	24	6	0.0	22–30	>2× weekly	chronic	(Hunt and Jones, 1980)
Ohlsson_1980	Intravenous	5 mg	4	11	0.0	18–35	frequent and occasional	chronic	(Ohlsson et al., 1980)
Lindgren_1981a	Intravenous	5 mg	4	18	11.1	19–36	daily	chronic	(Lindgren et al., 1981)
Lindgren_1981b	Intravenous	5 mg	4	18	11.1	19–36	<1× month	casual	(Lindgren et al., 1981)
Ohlsson_1982a[a]	Intravenous	5 mg	48	5	0.0	18–35	daily	chronic	(Ohlsson et al., 1982)
Ohlsson_1982b[a]	Intravenous	5 mg	48	4	0.0	18–35	<1× month	casual	(Ohlsson et al., 1982)
Kelly_1992a	Intravenous	5 mg	8	4	0.0	24–45	daily	chronic	(Kelly and Jones 1992)
Kelly_1992b	Intravenous	5 mg	8	4	0.0	24–45	<2 to 3× month	casual	(Kelly and Jones 1992)
Naef_2004[b]	Intravenous	0.053 mg/kg	8	4	50.0	26–35	naïve users	naïve	(Naef et al., 2004)
Morrison_2009	Intravenous	2.5 mg	2	22	0.0	28 ± 6	2–1000 episodes over last 10 years	casual	(Morrison et al., 2009)
Barkus_2011	Intravenous	2.5 mg	2	10	0.0	26 ± 4	324 exposures over last 24 years	casual	(Barkus et al., 2011)
Ohlsson_1980	Inhalation	13 mg	3	11	0.0	18–35	frequent and occasional	chronic	(Ohlsson et al., 1980)
Barnett_1981	Inhalation	8.94 mg	2	6	50.0	25–31	frequent users	chronic	(Barnett et al., 1982)
Lindgren_1981a	Inhalation	13.4 mg	2	18	11.1	19–36	<1× month	casual	(Lindgren et al., 1981)
Lindgren_1982b	Inhalation	12.7 mg	2	18	11.1	19–36	daily	chronic	(Lindgren et al., 1981)
Ohlsson_1982a	Inhalation	10 mg	48	4	0.0	18–35	<1× month	casual	(Ohlsson et al., 1982)
Ohlsson_1982b	Inhalation	10 mg	48	5	0.0	18–35	daily	chronic	(Ohlsson et al., 1982)
Perez–Reyes_1982a	Inhalation	9.7 mg	6	6	50.0	26–32	4–12× month	chronic	(Perez-Reyes et al., 1982)
Perez-Reyes_1982b	Inhalation	12.8 mg	6	6	50.0	26–32	4–12× month	chronic	(Perez-Reyes et al., 1982)
Perez-Reyes_1982c	Inhalation	16 mg	6	6	50.0	26–32	4–12× month	chronic	(Perez-Reyes et al., 1982)
Johansson_1988	Inhalation	15 mg	360	3	0.0	No info	daily	chronic	(Johansson et al., 1988)
McBurney_1986	Inhalation	0.15 mg/kg	22	10	0.0	18–30	occasional users	casual	(McBurney et al., 1986)
Huestis_1992a	Inhalation	15.8 mg	168	6	0.0	29–36	2 to 3× week	chronic	(Huestis et al., 1992)
Huestis_1992b	Inhalation	33.8 mg	168	6	0.0	29–36	2 to 3× week	chronic	(Huestis et al., 1992)
Kauert_2007a	Inhalation	0.25 mg/kg	6	10	10.0	19–21	occasional users	casual	(Kauert et al., 2007)
Kauert_2007b	Inhalation	0.50 mg/kg	6	10	10.0	19–21	occasional users	casual	(Kauert et al., 2007)
Hunault_2008a	Inhalation	29.3 mg	8	18	0.0	18–33	2–9× month	chronic	(Hunault et al., 2008)
Hunault_2008b	Inhalation	49.1 mg	8	20	0.0	18–33	2–9× month	chronic	(Hunault et al., 2008)
Hunault_2008c	Inhalation	69.4 mg	8	20	0.0	18–33	2–9× month	chronic	(Hunault et al., 2008)
Toennes_2008a	Inhalation	0.5 mg/kg	8	12	33.3	20–27	<4× week	casual	(Toennes et al., 2008)
Toennes_2008b	Inhalation	0.5 mg/kg	8	12	25.0	20–31	>4× week	chronic	(Toennes et al., 2008)
Schwope_2011a	Inhalation	54 mg	22	10	10.0	19–46	2× month	casual	(Schwope et al., 2011)
Toennes_2011	Inhalation	0.4 mg/kg	4	19	26.3	19–38	heavy users	chronic	(Toennes et al., 2011)
Desrosiers_2014a	Inhalation	54 mg	30	14	28.6	19–38	<2× week	casual	(Desrosiers et al., 2014)
Desrosiers_2014b	Inhalation	54 mg	30	11	27.3	22–41	>4× week	chronic	(Desrosiers et al., 2014)
Hunault_2014a	Inhalation	29.3 mg	8	18	0.0	18–45	2–9× month	chronic	(Hunault et al., 2014)
Hunault_2014b	Inhalation	49.1 mg	8	20	0.0	18–45	2–9× month	chronic	(Hunault et al., 2014)
Hunault_2014c	Inhalation	69.4 mg	8	20	0.0	18–45	2–9× month	chronic	(Hunault et al., 2014)
Newmeyer_2017a	Inhalation	50.6 mg	3.5	9	33.3	21–46	2–8× month	casual	(Newmeyer et al., 2017)
Newmeyer_2017b	Inhalation	50.6 mg	3.5	11	18.2	19–38	daily	chronic	(Newmeyer et al., 2017)

[a]Used for training the THC PBPK model for intravenous administration of THC. All other intravenous datasets were used for verification of the intravenous THC PBPK model.
[b]Used for training of the 11-OH-THC PBPK model. To note, this is the only dataset of 11-OH-THC formation after intravenous administration of THC. The 11-OH-THC PBPK model was verified with datasets after inhalation of THC, as described in the Methods section.
[c]Unless otherwise designated in the original reference, designation of naïve, casual, or chronic cannabis users was given to no previous cannabis use, cannabis use less than or greater than approximately twice a week, respectively.

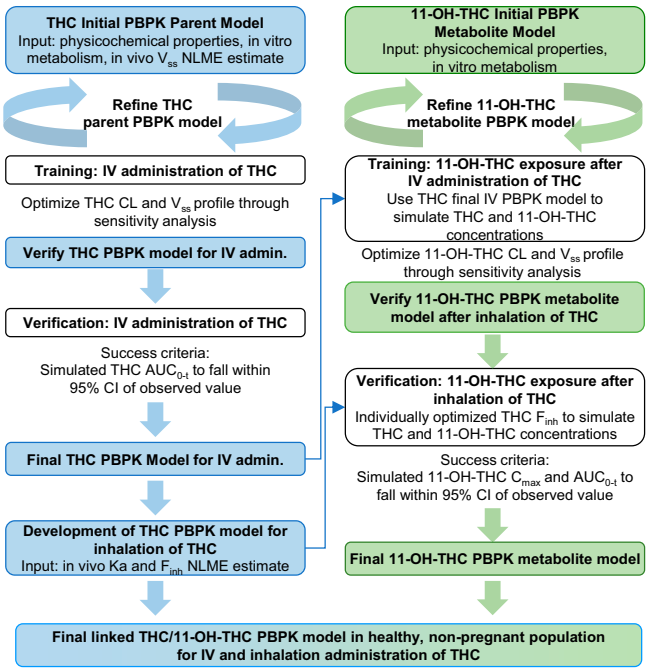

Fig. 1. General workflow of THC and 11-OH-THC PBPK model development and verification after intravenous and inhalation of THC in a healthy nonpregnant population.

Reyes, 1981). Within Simcyp, the Rodgers and Rowland method (Simcyp method 2) was selected for predicting tissue distribution because both THC and 11-OH-THC are neutral lipophilic compounds. The Rodgers and Rowland method accounts for binding to extracellular neutral lipids and neutral phospholipids and the affinity constant for binding to extracellular lipoproteins is predicted from the observed plasma unbound fraction (fu_p) and the blood-to-plasma (B/P) ratio. To match the predicted PBPK V_{ss} to the NLME estimated V_{ss} for THC, we elected to use a manually identified Kp scaler of 0.004. Such a Kp scaler was necessary because the Rodgers and Rowland method tends to overestimate V_{ss} for highly lipophilic compounds (Haddad et al., 2000; Rodgers and Rowland, 2007).

Data after intravenous administration of THC from Ohlsson et al., 1982 was used as the training dataset for the THC PBPK model. This dataset was chosen because it had the longest sampling time of 48 hours. As described above, and shown in Supplemental Fig. 2F, sampling times greater than 12 and 56 hours are necessary to accurately estimate the THC CL and V_{ss}, respectively. The THC intravenous PBPK model was verified using the remaining datasets after intravenous administration of THC.

Simulations of THC plasma/serum concentrations after inhalation of THC were conducted using the THC intravenous PBPK model with NLME estimated absorption parameters (ka and F_{inh}). To note, no change was made in the NLME model for chronic versus casual cannabis users. Furthermore, optimization of THC F_{inh} in the PBPK model for casual and chronic users was conducted via manual sensitivity analysis. Identification of the optimum THC F_{inh} was driven primarily by the observed THC plasma/serum AUC_{0-t} and not C_{max}, since AUC_{0-t} after THC inhalation was deemed a more robust parameter during model optimization.

To note, no THC parameters required optimization during the initial THC PBPK model development. During the development of the 11-OH-THC metabolite PBPK model, the 11-OH-THC fu_p was lowered via manual sensitivity analysis (further explanation below). We believed THC fu_p may have also been overpredicted, since THC fu_p was measured via the same methodology as 11-OH-THC. Since THC AUC_{0-t} after intravenous administration or inhalation of THC was not sensitive to changes to fu_p (because THC clearance is hepatic blood flow limited), we used the Simcyp prediction toolbox to estimate THC fu_p. This change was incorporated in the final THC PBPK model.

11-OH-THC PBPK Model Training and Verification in Healthy Nonpregnant Population. Development of 11-OH-THC metabolite PBPK model is shown in Fig. 1. Input values for the final 11-OH-THC PBPK model are listed in Table 1. As for THC, physicochemical properties were collected from literature. Due to similar high lipophilicity, we assumed the same percentage of 11-OH-THC bound to lipoprotein (63%) as THC. The Rodgers and Rowland method (Simcyp method 2), using a lipid binding scaler, was used to predict 11-OH-THC distribution. The lipid binding scaler (ψ) back calculates the maximum extent of cellular lipid binding by correlating neutral lipid and neutral phospholipid binding in red blood cells to that in tissue. Since there was no available observed quality data on 11-OH-THC V_{ss} to enable a similar strategy as for THC V_{ss}, and the Rodgers and Rowland prediction method greatly overestimates V_{ss} for compounds with $logP_{o:w} > 4$ (Haddad et al., 2000; Rodgers and Rowland, 2007), the lipid binding scaler was a reasonable alternative adjustment for predicting 11-OH-THC V_{ss}.

We have previously quantified the enzyme kinetics for 11-OH-THC clearance in vitro (Table 2) and found that UGT enzymes (fm = 0.60), CYP3A4 (fm = 0.18), and CYP2C9 (fm = 0.15) are the drug metabolizing enzymes responsible for hepatic metabolism of 11-OH-THC (Patilea-Vrana and Unadkat, 2019). Renal and biliary clearance were set to 0 l/h for 11-OH-THC. There is negligible excretion of unchanged 11-OH-THC in the urine, but up to 20% of radiolabeled 11-OH-THC dose is excreted unchanged in feces (Lemberger et al., 1972, 1973). However, the unchanged 11-OH-THC in feces may be 11-OH-THC deconjugated by bacterial β-glucuronidases. Furthermore, there is no current information on the extent (if any) of transport of 11-OH-THC by biliary efflux transporters, such as P-gp or BCRP.

The only datasets where 11-OH-THC was administered (as a parent) used TLC to quantify 11-OH-THC plasma concentrations(Lemberger et al., 1972a, 1973). For the reasons outlined above, these datasets were not considered further. There was only one remaining dataset with measured 11-OH-THC concentrations after intravenous administration of THC (Naef et al., 2004) available for 11-OH-THC PBPK model training. Due to this limitation, the 11-OH-THC PBPK metabolite model was optimized using observed 11-OH-THC data after intravenous administration of THC, and then verified using the observed 11-OH-THC plasma/serum concentration-time data after THC inhalation. Since the THC inhalation PBPK model was unable to be verified, THC F_{inh} was optimized for each inhalation dataset so that the observed THC plasma/serum AUC_{0-t} and C_{max} approximated the observed THC values. An optimized THC F_{inh} was necessary to ensure that the AUC and concentration-time profile of the parent compound (THC) was well characterized to verify the disposition of the metabolite (11-OH-THC).

During model development, 11-OH-THC AUC_{0-t} after administration of THC was initially underestimated. To recapitulate observations, we considered the following parameters for optimization to increase the simulated 11-OH-THC AUC_{0-t} after administration of THC: increase formation (fm) via CYP2C9, decrease 11-OH-THC intrinsic clearance (CL_{int}), increase fraction unbound in human liver microsome incubation (fu_{inc}), and decrease 11-OH-THC fu_p. We chose to optimize 11-OH-THC fu_p because this was a sensitive parameter that was experimentally derived and one for which we had the lowest confidence.

PBPK Model Verification and Performance Assessment. For each verification dataset, 10 trials were run, and the trial design was set to match the number of subjects, age range, and proportion of females as shown in Table 1. The simulated PK parameters needed to be within the 95% confidence interval of the observed value to meet our success criteria. Since all the observed studies had small sample size (<30 subjects), a t-distribution was used to calculate the 95% confidence interval. THC and 11-OH-THC PBPK model verification was performed by comparing observed and simulated THC AUC_{0-t} after intravenous administration of THC, and 11-OH-THC C_{max} and 11-OH-THC AUC_{0-t} after THC inhalation. Of note, no success criteria were assigned to THC AUC_{0-t} and C_{max} after THC inhalation because F_{inh} was individually optimized to verify the 11-OH-THC PBPK metabolite model. Bias and precision were calculated via the mean relative error (MRE) and relative root mean square error (rRMSE) as shown in Eq. 1 and 2, respectively (Sheiner and Beal, 1981).

$$MRE = \frac{1}{n}\sum_{i=1}^{n}\frac{(Pred_i - Obs_i)}{Obs_i} \times 100 \quad (1)$$

$$rRMSE = \sqrt{\frac{1}{n}\sum_{i=1}^{n}\left(\frac{Pred_i - Obs_i}{Obs_i}\right)^2} \times 100 \quad (2)$$

Extrapolation of THC and 11-OH-THC PBPK Model from Healthy Nonpregnant Population to Pregnant Women. The THC/11-OH-THC PBPK model verified in a healthy nonpregnant population (Fig. 1) was

TABLE 2

Drug dependent parameters of THC and 11-OH-THC used for PBPK M&S

Parameter	THC	Reference	11-OH-THC	Reference
Physicochemical properties				
Molecular weight (*g/mol*)	314.5	ChEMBL	330.5	ChEMBL
Log of octanol:water partition coefficient ($\log P_{o:w}$)	6.97	(Thomas et al., 1990)	5.33	(Thomas et al., 1990)
Compound type	Neutral	ChEMBL	Neutral	ChEMBL
Blood-to-plasma (B:P) ratio	0.667[b]	(Giroud et al., 2001)	0.625	(Giroud et al., 2001)
fu_p	0.0022	Predicted using Simcyp Prediction Toolbox	0.0050	Optimized via manual sensitivity analysis
Plasma binding proteins	HSA & lipoprotein (63% bound)	(Klausner et al., 1975)	HSA & lipoprotein (63% bound)	Assumed same lipoprotein binding as THC
Distribution – full PBPK model				
V_{ss} (*l/kg*)	6.5	Estimated using NLME model (Supplemental Figure 1)	3.8	Predicted via Rodgers and Rowland (Simcyp Method 2)
Kp scaler	0.004	Adjusted to match V_{ss}. Kp values predicted via Rodgers and Rowland (Simcyp Method 2)	N/A	—
Lipid binding scaler (ψ)	N/A	—	0.059	Predicted using Simcyp Prediction Toolbox
Lung ka (hr^{-1})	12	Estimated using NLME model (Supplemental Figure 1)	N/A	—
Lung F_{inh}	0.22	Estimated using NLME model (Supplemental Figure 1)	N/A	—
Elimination – enzyme kinetics				
CYP2C9 V_{max1} (*pmol/min/mg*) metabolite formed: 11-OH-THC	624	(Patilea-Vrana and Unadkat, 2019)	N/A	—
CYP2C9 K_{m1} (μM) (fu_{inc})	0.07 (0.04)	(Patilea-Vrana and Unadkat, 2019)	N/A	—
CYP2C9 V_{max2} (*pmol/min/mg*) metabolite formed: COOH-THC	N/A	—	4.83	(Patilea-Vrana and Unadkat, 2019)
CYP2C9 K_{m2} (μM) (fu_{inc})	N/A	—	0.50 (0.06)	(Patilea-Vrana and Unadkat, 2019)
CYP2C9 V_{max3} (*pmol/min/mg*) metabolite formed: unknown	N/A	—	54.4	(Patilea-Vrana and Unadkat, 2019)
CYP2C9 K_{m3} (μM) (fu_{inc})	N/A	—	0.50 (0.06)	(Patilea-Vrana and Unadkat, 2019)
CYP3A4 V_{max} (*pmol/min/mg*)	4905	(Patilea-Vrana and Unadkat, 2019)	1826	(Patilea-Vrana and Unadkat, 2019)
CYP3A4 K_m (μM) (fu_{inc})	5.48 (0.04)	(Patilea-Vrana and Unadkat, 2019)	12.8 (0.06)	(Patilea-Vrana and Unadkat, 2019)
Additional HLM CL (UGTs)[a] CL_{int} ($\mu l/min/mg$) (fu_{inc})	N/A	—	537 (0.06)	(Patilea-Vrana and Unadkat, 2019)
CL_R (*l/hr*)	0	(Wall and Perez-Reyes, 1981)	0	(Lemberger et al., 1972a)
CL_{bile} (*l/hr*)	0	(Wall and Perez-Reyes, 1981)	0	(Lemberger et al., 1972a)

[a]We have previously shown that UGT1A9 and UGT2B7 deplete 11-OH-THC using recombinant enzymes, but were unable to differentiate their fractional contributions due to the lack of selective inhibitors (Patilea-Vrana et al., 2018).

[b]To note, the THC blood-to-plasma (B:P) ratio reported by Giroud et al., 2001 was chosen over the reported THC B:P of 0.39 by Schwilke et al., 2009 because the latter required an adjustment of the hematocrit to 0.61 within the PBPK model, which is outside of the range of hematocrit levels for healthy individuals.

HLM, human liver microsome; N/A, not applicable.

extrapolated to pregnant women by incorporating gestational age–dependent physiologic changes. Based on phenytoin (a CYP2C9 substrate), pharmacokinetic data in pregnant and nonpregnant women, as well as PBPK modeling, our laboratory has determined that CYP2C9 activity increases 40%, 50%, and 60% during the first (T1), second (T2), and third trimester (T3), respectively (Ke et al., 2014). Based off midazolam (CYP3A4 substrate) pharmacokinetics in pregnant and nonpregnant women as well as in vitro studies and PBPK modeling, our laboratory has shown that CYP3A4 activity increases 100% throughout pregnancy (T1–T3) (Hebert et al., 2008; Ke et al., 2012; Zhang et al., 2015). There is no significant change in zidovudine (a UGT2B7 substrate) pharmacokinetics during pregnancy, suggesting there is no increase in UGT2B7 activity during pregnancy (O'Sullivan et al., 1993). Because the change, if any, in UGT1A9 activity during pregnancy is unknown, it was assumed to be unaffected during pregnancy (Anderson, 2005; Tasnif et al., 2016).

The final linked THC/11-OH-THC PBPK model developed for a healthy nonpregnant population was used to simulate disposition of THC and 11-OH-THC after inhalation of THC in pregnant women using the Simcyp virtual pregnancy population. Within the virtual pregnancy population, CYP2C9 expression was increased by 40%, 50%, and 60%, and CYP3A4 expression was increased 100%, 100%, and 100% for T1, T2, and T3, respectively. The trial design consisted of 10 trials with 10 subjects per trial of women age 20-45 at gestational weeks (GWs) 12, 26, and 40 to represent T1, T2, and T3, respectively.

To our knowledge, only one human clinical study has reported serum concentrations of THC and 11-nor-9-carboxy-Δ^9-THC (COOH-THC), the main secondary and nonpsychoactive metabolite of THC, in maternal and umbilical cord blood at delivery (Blackard and Tennes, 1984). Concentrations of 11-OH-THC were not reported by Blackard and Tennes, 1984. This study used GC-MS to measure THC concentrations, and per our criteria defined earlier, we considered

the data to be analytically robust. Ten subjects who smoked cannabis daily during the third trimester participated in the study. Information on the time since last smoking cannabis was provided, but the THC dose was not. The THC dose the subjects may have inhaled was calculated by multiplying the average percentage of THC (weight/weight) (ElSohly et al., 2000) in 1984 (the year the study was conducted) with the average weight of a joint (Mariani et al., 2011). The THC dose was approximated to be 21.8 mg. Simulations were performed using F_{inh} of 0.35, a value estimated for chronic cannabis use during the PBPK model development after inhalation of THC.

Fetal serum concentrations of THC were simulated using a maternal-fetal PBPK (m-f-PBPK) model previously described (Zhang et al., 2017; Zhang and Unadkat, 2017). Since maternal THC serum concentrations drive fetal serum concentrations, adjustments were made to the THC dose for each subject, so the simulated maternal THC serum concentrations matched the observed data. Due to high lipophilicity, it was assumed THC is placental blood flow limited and, as such, the placental passive diffusion clearance was set to 500 l/h. Placental or fetal THC metabolism was assumed to be negligible. The simulations were first run with no placental efflux transport, and simulated fetal-to-maternal (F/M) serum concentrations were compared with observed data. Due to an overprediction of THC F/M ratio, we explored the impact of placental efflux transport required to recapitulate the observed fetal data. To match the observed fetal concentrations, the fraction transported (ft) via active placental efflux (expressed as a fraction of active efflux to active efflux plus passive diffusion clearance) was adjusted so that the simulated fetal THC serum concentrations matched the observed values.

Results

THC V_{ss} and Inhalation Absorption Kinetics Estimates via NLME Model. THC $V_{ss,}$ estimated via an NLME model using the mean concentration data from 11 datasets after intravenous administration of THC was 6.5 l/kg (39% RSE). The NLME model estimates for THC ka and F_{inh}, estimated using the mean concentration data from 29 datasets after inhalation of THC, was 12 (12% RSE) min^{-1} and 0.22 (33% RSE), respectively. The goodness-of-fit plot in Supplemental Fig. 2 shows good model fit of the observed THC plasma/serum concentrations after intravenous and inhalation of THC.

THC PBPK Model Development and Verification in Healthy Nonpregnant Population. The in vitro to in vivo extrapolation of THC and 11-OH-THC enzyme kinetics based on our previous quantification was successful (Patilea-Vrana and Unadkat, 2019). The only PBPK model optimization performed was adjustment of THC fu_p from 0.011 to 0.0022 and 11-OH-THC fu_p from 0.012 to 0.0050. The final PBPK model input parameters used are shown in Table 2.

During model verification after intravenous administration of THC, the PBPK model–predicted THC plasma $AUC_{0\text{-}t}$ met our success criteria for seven out of eight datasets (Table 3). For the Lindgren_1981a dataset, the simulated plasma $AUC_{0\text{-}t}$ was underestimated, however, it was close to the 95% confidence interval limit. Nevertheless, all simulated THC plasma $AUC_{0\text{-}t}$ were within 2-fold of the observed value (Table 3). The bias (MRE) and precision (rRMSE) for the predicted THC $AUC_{0\text{-}t}$ after intravenous administration of THC were −6% and 20%, respectively. Overall, the predicted THC plasma concentration-time profiles were similar to the observed profiles, with 70% of the simulated values within 2-fold of the observed values (Supplemental Fig. 3). Given the success criteria, bias and precision, the THC PBPK intravenous model performed well.

Using the verified THC intravenous PBPK model and the NLME estimates for THC inhalation absorption (ka = 12 $hour^{-1}$ and F_{inh} = 0.22, see Supplemental Fig. 2), THC plasma/serum $AUC_{0\text{-}t}$ and C_{max} after inhalation of THC were simulated and compared with observed data (Supplemental Fig. 4). Of the 27 THC inhalation datasets, 13 did not meet the success criteria for $AUC_{0\text{-}t}$ (Supplemental Table 3). Interestingly, there was very little bias (MRE = 1%) but poor precision (rRMSE = 88%). This was in part because THC plasma/serum $AUC_{0\text{-}t}$ and C_{max} were generally overpredicted for casual cannabis users and underpredicted for chronic users (Fig. 2, A and B). For these reasons, the THC inhalation PBPK model could not be verified. For any simulated THC plasma/serum $AUC_{0\text{-}t}$ that did not initially fall within the 95% confidence interval of the observed value, F_{inh} was manually optimized to approximate the observed THC $AUC_{0\text{-}t}$ value (Supplemental Table 3). As shown in Fig. 2C, chronic users had a higher F_{inh} compared with casual users (mean ± S.D. F_{inh} = 0.35 ± 0.19 and 0.19 ± 0.14, respectively).

11-OH-THC PBPK Model Development and Verification in Healthy Nonpregnant Population. The 11-OH-THC PBPK model was developed using the only available dataset that measured 11-OH-THC plasma concentrations after THC intravenous administration (Naef et al., 2004) (Supplemental Fig. 3C) and then verified using datasets that measured 11-OH-THC plasma/serum concentrations after inhalation of THC using optimized THC F_{inh} (Supplemental Fig. 4; Supplemental Table 3**;** Table 4). Twelve out of the 16 simulated 11-OH-THC plasma/serum C_{max} met the success criteria, whereas 12 out of 14 simulated 11-OH-THC plasma/serum $AUC_{0\text{-}t}$ met the success criteria (Table 4). To note, the two datasets from Newmeyer et al., 2017 only reported 11-OH-THC blood C_{max} and not $AUC_{0\text{-}t}$. For the prediction of plasma/serum concentrations of 11-OH-THC, the bias and precision were as follows: 87% and 151% for C_{max} and 15% and 60% for $AUC_{0\text{-}t}$, respectively. As shown in Fig. 2D, although 11-OH-THC C_{max} tended to be overestimated, all the values (except for the Newmeyer_2017a dataset) were within 2-fold of the observed C_{max}. Furthermore, as shown in Fig. 2E, except for the Huestis_1992b dataset, all the simulated $AUC_{0\text{-}t}$ were within 2-fold of the observed values. Due to these outliers, the precision for 11-OH-THC C_{max} and $AUC_{0\text{-}t}$ was

TABLE 3

Verification of THC PBPK model after intravenous administration of THC

The PBPK-simulated plasma THC $AUC_{0\text{-}t}$ from Lindgren_1981a dataset did not fall within the 95% confidence interval of observed value (bolded value) and thus did not meet the success criteria. Because THC was administered intravenously, the success criteria for the THC PBPK model included only plasma $AUC_{0\text{-}t}$ and not C_{max}.

Study	Cannabis User	THC $AUC_{0\text{-}t}$			
		Simulated	Observed	Observed 95% CI Limits	
		*ng*hr/ml*			
Hunt_1980	chronic	32	26	17	34
Ohlsson_1980	chronic	64	60	57	64
Lindgren_1981a	chronic	**64**	81	65	96
Lindgren_1981b	casual	64	58	47	68
Kelly_1992a	chronic	76	101	49	153
Kelly_1992b	casual	76	122	48	196
Morrison_2009	casual	28	31	28	34
Barkus_2011	casual	28	29	24	35

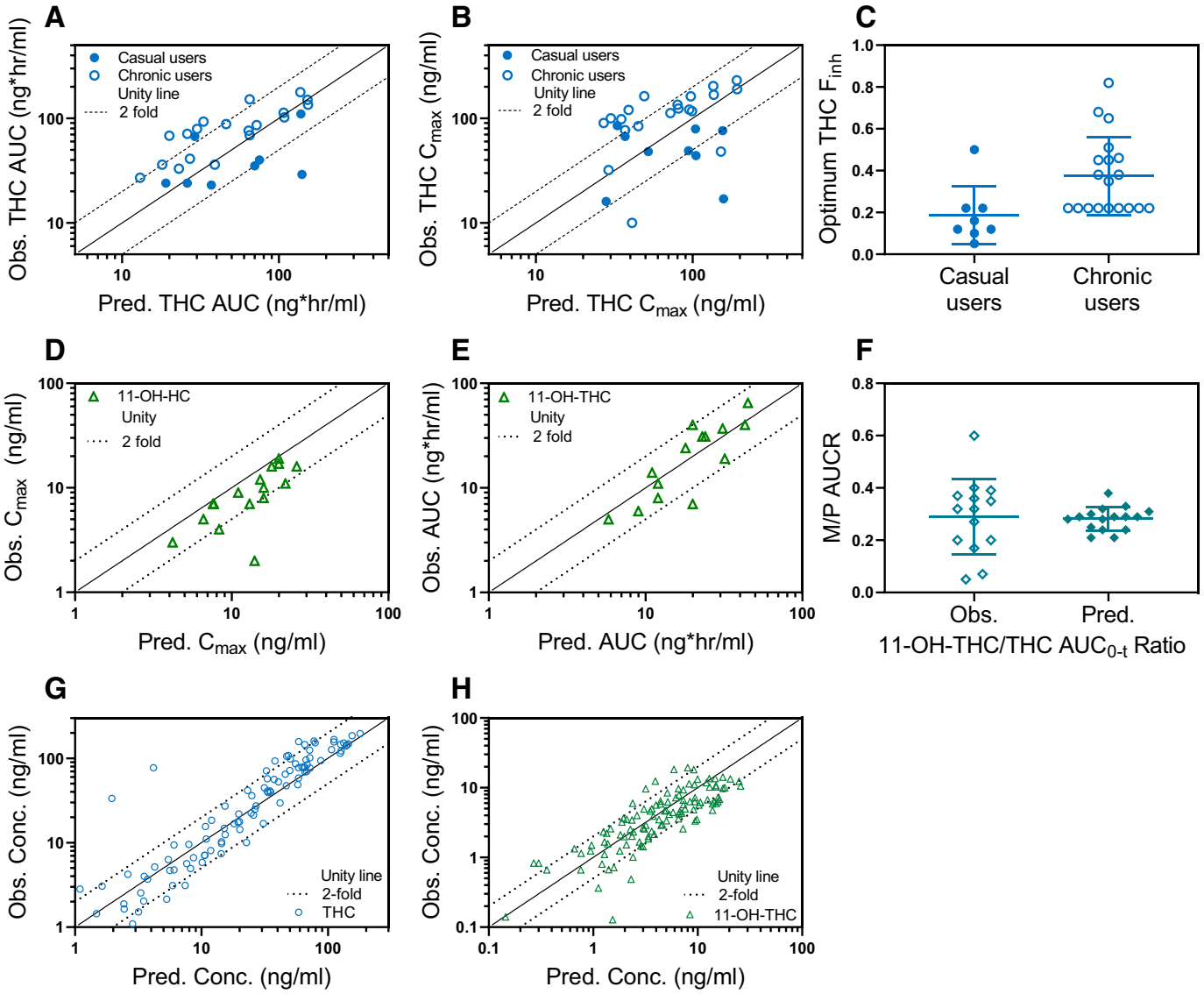

Fig. 2. Observed (Obs.) and PBPK model–predicted (Pred.) THC plasma or serum (A) $AUC_{0\text{-}t}$ and (B) C_{max} after inhalation of THC. The final THC intravenous PBPK model predictions (A and B) used the NLME estimated absorption parameters (ka = 12 $hour^{-1}$ and F_{inh} = 0.22). The THC $AUC_{0\text{-}t}$ and C_{max} for casual users was typically overpredicted, whereas the reverse was true for chronic users. This suggests that casual and chronic users require a lower and higher F_{inh}, respectively. (C) THC F_{inh} was optimized for chronic and casual users via manual adjustment in order for datasets to meet the success criteria for the THC inhalation PBPK model. The optimized average ± S.D. F_{inh} were 0.19 ± 0.14 and 0.35 ± 0.19 for casual and chronic users, respectively. Using these optimized THC F_{inh}, the PBPK model–-predicted versus observed parameters for 11-OH-THC after inhalation of THC are shown in (D–H). (D) The predicted 11-OH-THC C_{max} was larger than that observed but typically within 2-fold of observed values. (E) Majority of the predicted 11-OH-THC $AUC_{0\text{-}t}$ fell within 2-fold of the observed values. (F) The mean simulated 11-OH-THC to THC $AUC_{0\text{-}t}$ ratios (M/P AUCR) were similar to the observed values, indicating that the 11-OH-THC final PBPK model performed well. (G) Since the THC F_{inh} was optimized for each dataset, majority of the THC predicted concentrations were within 2-fold of observed values. (H) Majority of the predicted 11-OH-THC concentrations after THC inhalation were within 2-fold of observed values, further indicating good performance of the 11-OH-THC PBPK model.

worsened. Further inspection showed good agreement between the simulated versus observed mean ± S.D. 11-OH-THC/THC plasma AUC ratio (M/P AUCR) of 0.29 ± 0.05 and 0.29 ± 0.15, respectively (Fig. 2F). Overall, the simulated 11-OH-THC plasma/serum concentrations were comparable to the observed values, however, there was variability among the studies. Indeed, 80% and 79% of the simulated THC and 11-OH-THC plasma/serum concentrations, respectively, were within 2-fold of the observed value (Fig. 2, G and H). Pooling together the success criteria, bias, precision, and the additional PBPK model performance, the 11-OH-THC PBPK model performed well.

Using the final linked THC/11-OH-THC PBPK model, sensitivity analysis was performed to identify parameters that impact THC CL, THC V_{ss}, and M/P AUCR (Fig. 3). THC predicted plasma CL was 57 l/h (blood CL of 86 l/h), making THC a high clearance compound. Since THC clearance is blood flow limited, THC CL was not sensitive to changes in total CL_{int}, fu_p, or fu_{inc}. Due to high lipophilicity, THC V_{ss} was most sensitive to fu_p and distribution into the adipose. As anticipated, the metabolite (11-OH-THC) to parent (THC) AUC ratio (M/P AUCR) was sensitive to changes in 11-OH-THC formation (fm and THC CL_{plasma}) and changes to 11-OH-THC elimination (11-OH-THC CL_{int}). A sensitivity analysis was performed for fu_{inc} since the CL_{int} values used in the PBPK model are in vitro observed values adjusted for microsomal binding and, therefore, errors in fu_{inc} will reflect in error in total CL_{int} values. To reflect potential errors in CL_{int} due to fu_{inc}

TABLE 4

Verification of 11-OH-THC PBPK model after inhalation of THC

PBPK-simulated parameters in bold did not fall within the 95% confidence interval of observed value and thus did not meet the success criteria. Since the 11-OH-THC (metabolite) PBPK model was verified with data after inhalation of THC, THC F_{inh} was manually optimized to ensure exposure of the THC (parent) was well predicted (see Supplemental Table 3 for optimum THC F_{inh} for each dataset). As such, THC C_{max} and $AUC_{0\text{-}t}$ after inhalation of THC could not be verified (see further explanation in Methods section).

Study	Cannabis User	11-OH-THC C_{max}				11-OH-THC $AUC_{0\text{-}t}$			
		Sim.	Obs.	95% CI or Range[b] of Observed		Sim.	Obs.	95% CI or Range[b] of Observed	
		ng/ml				*ng*hr/ml*			
McBurney_1986	casual	20	19	10	28	**20**	40	23	57
Huestis_1992a	chronic	7.6	6.7	3.3[b]	10[b]	9	5.7	NC	NC
Huestis_1992b	chronic	16	7.5	3.8[b]	16[b]	20	7.2	NC	NC
Kauert_2007a	casual	**4.2**	2.5	1.4	3.6	5.8	4.6	2.7	6.5
Kauert_2007b	casual	**8.3**	3.6	2.0	5.2	**12**	8.0	5.0	11
Hunault_2008a	chronic	11	9.2	5.4	13	18	24	16	32
Hunault_2008b	chronic	18	16	9.3	23	31	37	25	48
Hunault_2008c	chronic	**26**	16	12	20	43	40	31	49
Toennes_2008a	casual	7.7	6.7	3.5	9.9	11	14	9.6	18
Toennes_2008b	chronic	15	12	5.4	19	23	31	16	46
Schwope_2011	casual	16	10	4.0[b]	16[b]	32	19	7.5[b]	42[b]
Toennes_2011	chronic	20	17	12	22	24	31	20	42
Desrosiers_2014a	casual	6.6	5.3	0.0[b]	16[b]	12	11	0.9[b]	36[b]
Desrosiers_2014b	chronic	22	11	3.6[b]	26[b]	45	65	20[b]	106[b]
Newmeyer_2017a	casual	**14**[a]	1.9[a]	0.5[a]	8.7[a]	16[a]	NR	NR	NR
Newmeyer_2017b	chronic	13[a]	7.2[a]	1.9[a]	31[a]	16[a]	NR	NR	NR

[a]PBPK simulated and observed blood C_{max} and $AUC_{0\text{-}t}$. All other measurements are plasma or serum values.
[b]The 95% CI of the observed values could not be calculated for the following datasets since S.D. was not reported; instead, the range (min–max) of the observed parameter are listed: Huestis et al., 1992, Schwope et al., 2011, Desrosiers et al., 2014, Newmeyer et al., 2017.
NC: 95% confidence interval not calculated since $AUC_{0\text{-}t}$ was estimated via noncompartmental analysis of the digitized average concentrations.
NR: 11-OH-THC $AUC_{0\text{-}t}$ not reported by Newmeyer et al., 2017.

measurements, fu_{inc} was changed by the same proportion for both THC and 11-OH-THC in the sensitivity analysis, which effectively changed the THC and 11-OH-THC CL_{int} by the same proportion. As shown in Fig. 3, fu_{inc} impacts THC and 11-OH-THC disproportionally, since fu_{inc} and therefore CL_{int} was a sensitive parameter to M/P AUCR but not THC CL. To further explain the impact on M/P AUCR, a simulation was run where the fu_pCL_{int} of THC and 11-OH-THC were decreased by 10 or 100-fold, whereas fm and 11-OH-THC CL_{int} formation-to-elimination ratio was maintained the same (Supplemental Table 4). 11-OH-THC plasma AUC decreased proportional to its formation CL_{int}, whereas THC plasma AUC did not change proportionally to its CL_{int}.

Extrapolation of THC and 11-OH-THC PBPK Model From Healthy Nonpregnant Population to Pregnant Women. Gestational age–dependent changes were applied to the final linked THC/11-OH-THC PBPK model verified in healthy nonpregnant population, and THC/11-OH-THC disposition was simulated at the end of T1 (GW = 12), T2 (GW = 26), and T3 (GW = 40). As shown in Fig. 4, A and B, the overall simulated THC plasma concentration-time profile or AUC

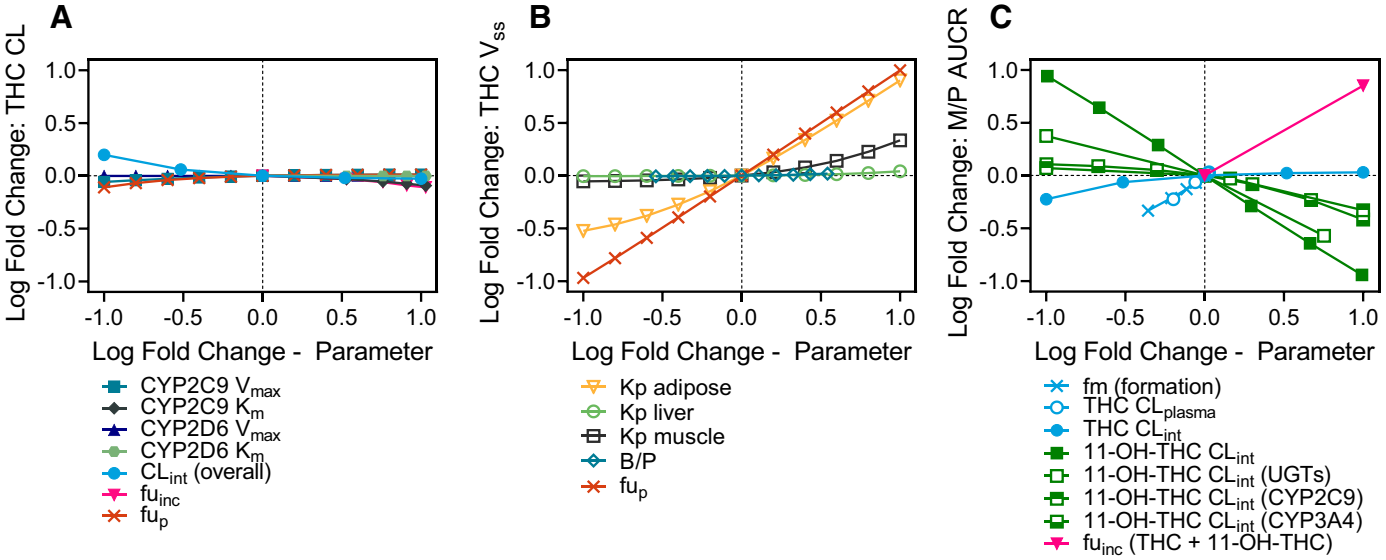

Fig. 3. Sensitivity analyses were conducted to assess impact of various PBPK model parameters on THC and 11-OH-THC disposition. (A) Since THC has high CL that is blood flow limited, THC CL is not sensitive to alterations to THC CL_{int} or protein binding (fu_p and fu_{inc}). (B) Since THC is a highly lipophilic compound, V_{ss} is most sensitive to fu_p and changes in the distribution of THC into adipose. (C) The 11-OH-THC to THC AUC ratio (M/P AUCR) is sensitive to changes in 11-OH-THC formation (fm and THC CL_{plasma}), 11-OH-THC elimination (11-OH-THC CL_{int}), and fu_{inc} estimate but the M/P AUCR is not sensitive to change in THC CL_{int}.

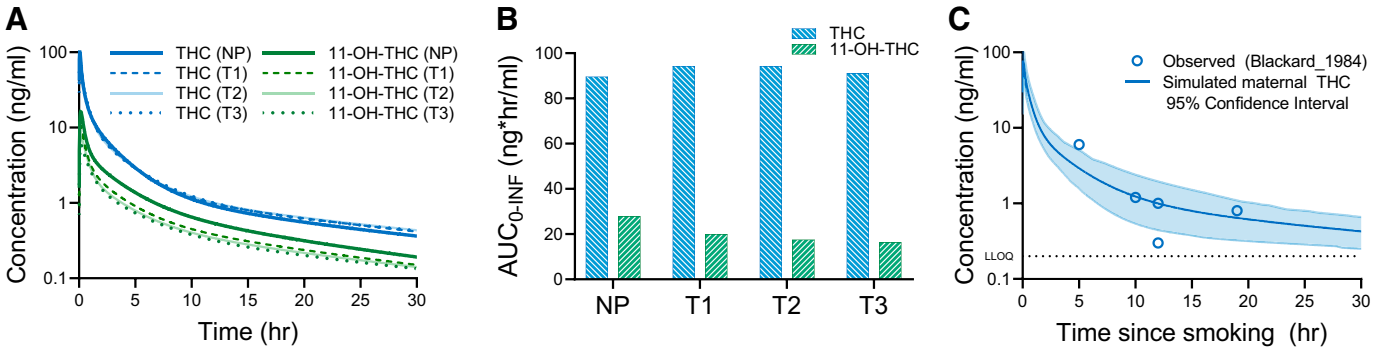

Fig. 4. PBPK model–predicted serum THC and 11-OH-THC (A) concentration-time profiles and (B) $AUC_{0\text{-inf}}$ in nonpregnant (NP) and pregnant [T1 (GW = 12), T2 (GW = 26), T3 (GW = 40)] subjects after inhalation of THC. (C) PBPK model–predicted and observed maternal serum THC concentrations at delivery (GW = 40) after smoking cannabis. To note, each datum represents an observed value from a different subject. These data are from Blackard and Tennes, 1984 and they did not report the dose of THC used by the subjects. As such, simulations were run assuming a dose representative of the average THC content in cannabis in 1984 (see *Materials and Methods* section).

did not change during pregnancy. The simulated plasma 11-OH-THC AUC decreased 28%, 37%, and 41% during T1, T2, and T3, respectively.

To investigate the impact of the gestational age–dependent physiologic changes on the observed THC and 11-OH-THC PK changes during pregnancy, a systematic sensitivity analysis was performed. As shown in Table 5, THC plasma AUC was not sensitive to any of the gestational age–dependent changes. 11-OH-THC plasma AUC was most sensitive to the increase in 11-OH-THC fu_p and increase in the cytochrome P450 enzyme expression (represented by increase in CYP3A4 and CYP2C9 V_{max}). Even though 50% increase in CYP2C9 activity led to 50% increase in the intrinsic formation clearance of 11-OH-THC (represented by THC CYP2C9 V_{max}), the overall fm to 11-OH-THC increased from 0.91 to 0.94. As such, the increase in intrinsic formation clearance of 11-OH-THC was not a sensitive parameter. Collectively, the simulated decrease in 11-OH-THC AUC during pregnancy was due to an increase in unbound elimination clearance of 11-OH-THC.

To test whether the extrapolation of THC from healthy nonpregnant to pregnant women was successful, THC plasma/serum concentrations were simulated after inhalation of an average joint with THC concentrations in cannabis reflective of that available in 1984 and compared with the observed data in pregnant women (Fig. 4C). Although dosing information is missing from Blackard and Tennes (1984), the simulated serum concentrations after inhalation of THC are comparable to the observed data. Although we cannot verify the THC PBPK model in pregnant women, we have confidence in the simulated output during pregnancy for THC and 11-OH-THC, since the methodology of extrapolating from healthy nonpregnant population to pregnant women has been verified by us for multiple drugs (Ke et al., 2012, 2014; Zhang and Unadkat, 2017).

THC fetal serum concentrations were simulated using a m-f-PBPK model. The dose for each subject was adjusted in order for the simulated THC maternal serum concentration to approximate the observed values. This was performed to ensure that maternal concentrations that drive fetal THC concentrations were well predicted. The observed THC F/M ratio for the three subjects with available data were 0.17, 0.25, and 0.38 (Supplemental Table 5). This suggests fetal exposure of THC is limited by placental efflux, placental metabolism, fetal metabolism, and/or placental sequestration. Indeed, simulations run in the absence of any placental and fetal metabolism/transport, the simulated F/M values overpredicted the observed values. Placental efflux (presumably by P-gp and/or BCRP) ft of 0.88, 0.92, and 0.93 was necessary to recapitulate the observed fetal THC serum concentrations (Supplemental Table 5).

Discussion

Several THC PBPK models in healthy nonpregnant populations have been previously developed. Wolowich et al., 2019 developed a linked THC/11-OH-THC/COOH-THC minimal PBPK (mPBPK) model for

TABLE 5

Sensitivity analysis of PK parameters impacted by gestational age–dependent physiologic changes during the third trimester

Sensitivity analysis was run in a nonpregnant population to demonstrate how the physiologic changes observed in pregnancy help explain the simulated changes in THC and 11-OH-THC plasma concentrations during pregnancy (Fig. 4). The input parameters are the fold PK changes caused by gestational age–dependent physiologic changes during the third trimester and are as follows: 50% and 100% increase in CYP2C9 and CYP3A4 activity, respectively, increase in THC and 11-OH-THC fu_p from 0.0022 to 0.0031 and 0.0050 to 0.0069 (as predicted by the PBPK simulation of THC and 11-OH-THC in a pregnant population by Simcyp at GW = 40 weeks). To note, although there is an increase in CYP2D6 activity during pregnancy (Anderson, 2005; Tasnif et al., 2016), no sensitivity analysis was run since CYP2D6 fm is small (fm = 0.09). Furthermore, no sensitivity analysis was run on UGT-mediated clearance of 11-OH-THC since expression of UGT2B7 or UGT1A9 does not change during pregnancy (Anderson, 2005; Tasnif et al., 2016).

Percent Change: Input Parameters						Percent Change: Output Parameters			
THC		11-OH-THC				THC		11-OH-THC	
CYP2C9 V_{max}	fu_p	CYP2C9 V_{max1}	CYP2C9 V_{max2}	CYP3A4 V_{max}	fu_p	C_{max}	$AUC_{0\text{-}t}$	C_{max}	$AUC_{0\text{-}t}$
↔	↔	↑50%	↑50%	↔	↔	↔	↔	↓5%	↓6%
↔	↔	↔	↔	↑100%	↔	↔	↔	↓14%	↓17%
↑50%	↔	↔	↔	↔	↔	↓1%	↓2%	↑6%	↑5%
↔	↔	↔	↔	↔	↑40%	↔	↔	↓26%	↓29%
↔	↑40%	↑50%	↔	↔	↔	↓10%	↓6%	↓12%	↓3%
↔	↔	↑50%	↑50%	↑100%	↔	↔	↔	↓18%	↓21%
↑50%	↔	↑50%	↑50%	↑100%	↔	↓1%	↓2%	↓13%	↓18%
↑50%	↔	↑50%	↑50%	↑100%	↑40%	↓1%	↓2%	↓36%	↓42%
↑50%	↑40%	↑50%	↑50%	↑100%	↑40%	↓11%	↓7%	↓44%	↓44%

THC intravenous and oral administration using a hybrid bottom-up and top-down approach. The authors attributed the CL_{int} of THC and 11-OH-THC entirely to CYP2C9, and they estimated these parameters by fitting the mPBPK model data after intravenous and oral (PO) administration of THC. Methaneethorn et al., 2020 developed a THC PBPK model for intravenous, PO, smoking, and vaporization of THC by extrapolating a previously developed PBPK model in mice, rats, and pigs to humans. The authors used observed values for systemic THC CL, and such, the PBPK model is not mechanistic. As detailed below, our THC/11-OH-THC PBPK model adds to the above contributions in several important ways. First, our PBPK model is built using a bottom-up approach that integrates full mechanistic PK information (such as metabolism of 11-OH-THC via CYP2C9, CYP3A, and UGTs). Second, we performed extensive verification of the THC and 11-OH-THC PBPK models in healthy nonpregnant population after intravenous and inhalation administration of THC. Finally, we are the first to use a THC/11-OH-THC PBPK model to predict the disposition of THC/11-OH-THC in pregnant women.

The meta-analysis of available THC data after intravenous administration and inhalation of THC provides insights previously not recognized. First, studies that used TLC to quantify THC and 11-OH-THC (Lemberger et al., 1970, 1971, 1972b; Wall et al., 1983) were different from the remaining studies, likely due to the nonspecific assay used to quantify cannabinoid plasma concentrations. Therefore, caution should be exercised when interpreting THC/11-OH-THC PK parameters from these studies. Second, NLME modeling of the mean THC concentrations from 25 different studies (40 datasets) that vary widely in sampling time window and sampling density allowed for the most comprehensive analysis of the population mean V_{ss}, F_{inh}, and ka of THC. Lastly, we showed that at least 12 and 56 hours are necessary to capture enough of THC PK profile to accurately calculate its CL and V_{ss}. That is, the large variability in THC reported PK parameters, especially V_{ss}, can be attributed, in part, to insufficient sampling time windows.

The foundation of our bottom-up approach was the extrapolation of in vitro mechanistic PK information previously quantified in vitro (Patilea-Vrana and Unadkat, 2019). The only parameters that required optimization during PBPK model building were fu_p of THC and 11-OH-THC, which were previously measured by us using ultracentrifugation (Patilea-Vrana and Unadkat, 2019). For drugs that are highly protein bound, it is possible that THC binding to lipoproteins (Klausner et al., 1975) and contamination of the unbound fraction from these lipoproteins led to an overestimation of fu_p (Brockman et al., 2015). Since THC CL_{int} exceeds hepatic blood flow, THC plasma CL is blood flow limited and not sensitive to changes in its CL_{int}. Therefore, the in vitro estimated THC CL_{int} could be several folds off, and the THC PBPK model would still perform well. The mean simulated and observed M/P AUCR after inhalation of THC were the same (Fig. 2F). This means that the combination of fm, 11-OH-THC CL_{int}, and fu_p estimates must be accurate. When considering the impact of CL_{int} on both THC and 11-OH-THC disposition as outlined above, we conclude that the in vitro to in vivo extrapolation of the mechanistic PK information previously quantified (Patilea-Vrana and Unadkat, 2019) was successful. Further PBPK model development using THC and 11-OH-THC disposition after oral administration of THC will help identify the accuracy of the extrapolated THC and 11-OH-THC CL_{int} values.

Initially, using the NLME estimates for F_{inh} of 0.22 and ka of 12 $hour^{-1}$, our PBPK model over- and underestimated plasma/serum THC $AUC_{0\text{-}t}$ and C_{max} for the casual and chronic users after THC inhalation, respectively. After optimization of F_{inh}, the average estimated F_{inh} for casual and chronic users was 0.19 and 0.35, respectively (Fig. 2C). Indeed, studies have observed an increase in THC plasma AUC after inhalation of THC in chronic versus casual users (Toennes et al., 2008; Desrosiers et al., 2014). Some have hypothesized that chronic users have an increased THC CL (Lemberger et al., 1971), but this is unlikely due to THC CL being blood flow limited. History of regular cannabis use is correlated with average volume inhaled per puff and puff volumes (McClure et al., 2012). Furthermore, chronic users develop a tolerance to the psychoactive effects of cannabis and require higher levels of THC to achieve the desired effect (Lee et al., 2013). Therefore, the different smoking topography and tolerance but not increase in THC CL between chronic and casual users likely leads to the difference in THC F_{inh}.

A seemingly paradoxical situation is observed regarding the formation kinetics of 11-OH-THC. The half-life of 11-OH-THC is similar to that of THC, suggesting formation-rate limited kinetics, however, the in vitro formation clearance of 11-OH-THC is much greater than its elimination clearance (Patilea-Vrana and Unadkat, 2019). Interestingly, Wolowich et al. (2019) invoked a hepatic sinusoidal diffusional barrier for THC to help explain this discrepancy in their mPBPK model. A sinusoidal diffusional barrier is unlikely given the high lipophilicity of THC. In our sensitivity analysis, we showed that proportional changes to CL_{int} of THC and 11-OH-THC impact THC CL and M/P AUCR disproportionally (Supplemental Table 4). This phenomenon can be explained by the M/P relationship, defined as: $\frac{M}{P} = \frac{fm*CL_{parent}}{fupCLint_{metabolite}}$ (Pang et al., 2008). The formation clearance of the metabolite, defined as $fm*CL_{parent}$, can become blood/plasma-flow limited, whereas the metabolite intrinsic elimination clearance, defined by $fu_p*CLint_{metabolite}$, cannot. As such, even though the in vitro intrinsic formation of 11-OH-THC is much greater than its elimination, 11-OH-THC has apparent formation-rate limited kinetics because THC hepatic CL is limited by hepatic blood/plasma flow. This helps explain why the observed M/P AUCR is less than unity, but THC and 11-OH-THC have similar in vivo half-lives.

To our knowledge, this is the first example of extrapolation of a PBPK model of THC/11-OH-THC during pregnancy. Previous studies from our laboratory demonstrated successful prediction of drugs, such as midazolam, indinavir, and glyburide, by extrapolating from healthy nonpregnant population to pregnant women using PBPK M&S (Ke et al., 2012, 2014). Using the same approach, exposure of THC and 11-OH-THC after inhalation of THC was extrapolated from the THC/11-OH-THC PBPK model verified in nonpregnant population to pregnant women by accounting for gestational age–dependent changes. Although we were unable to verify the THC predictions during pregnancy since the study by Blackard and Tennes (1984) lacked THC dosing information, the current extrapolation using average THC content in joints in 1984 was comparable with observed data (Fig. 4C). Simulations shown in Fig. 4 predict that during pregnancy, THC AUC does not change, whereas 11-OH-THC AUC decreases by up to 41% by T3. As predicted by sensitivity analysis in Table 5, changes to 11-OH-THC are mainly driven by the overall increase in 11-OH-THC fu_pCL_{int}, which is driven by an increase in both CYP2C9 and CYP3A4 activity and increase in plasma protein binding. Although the increase in CYP2C9 did not increase the THC fm to 11-OH-THC (0.91 to 0.94 for nonpregnant and T3, respectively), the impact may be more pronounced if this fm value was smaller. This may be true for subjects with CYP2C9 genetic polymorphism that confer decreased activity and therefore lower fm. However, it is unknown whether induction of polymorphic CYP2C9 during pregnancy is similar to that of the wild-type CYP2C9.

The observed THC F/M concentration ratios in humans ranged from 0.17 to 0.38 (Blackard and Tennes, 1984). A similar THC F/M ratio was observed in macaques (Bailey et al., 1987), indicating placental/fetal metabolism, placental efflux, and/or placental sequestration may limit exposure of THC to the fetus. Indeed, initial simulations assuming no placental and fetal metabolism or transport overestimated the THC F/M concentration ratio. Placental enzymes, including CYP1A1, UGT1A9, and UGT2B7, were observed to turn over THC and 11-OH-THC

(UGTs only) in recombinant enzyme studies (Patilea-Vrana et al., 2018). However, there was minimal depletion of THC and 11-OH-THC in human placental microsomes (data not shown). Since THC is a substrate of P-gp and BCRP (Bonhomme-Faivre et al., 2008; Spiro et al., 2012), we explored the theoretical active placental efflux needed to recapitulate the observed F/M ratios in the m-f-PBPK model. An average placental efflux ft of 0.91 was estimated via sensitivity analysis (Supplemental Table 5). Placental efflux ft ranging from 0.33 for tenofovir to 0.94 for paclitaxel have been previously observed for drugs that are substrates of P-gp or BCRP (Han et al., 2018). These data and our simulations suggest that placental efflux transport may play a role in limiting fetal exposure to THC. The magnitude of THC placental active efflux as well as additional mechanisms that may contribute to THC fetal exposure needs to be experimentally characterized. Since the placental expression of P-gp and BCRP varies with gestational age (Anoshchenko et al., 2020), and since prenatal use of THC at different stages of pregnancy can differentially impact neonatal outcomes (Grzeskowiak et al., 2020), it is important to understand the fetal exposure of THC throughout pregnancy. Further investigation into THC and 11-OH-THC placental metabolism and transport (or other reasons for this low F/M ratio) are ongoing in our laboratory to further refine the fetal THC and 11-OH-THC predictions.

Overall, a linked THC/11-OH-THC PBPK model was built and verified after intravenous administration and inhalation of THC in a healthy nonpregnant population. This PBPK model provides the mechanistic foundation that can be used to extrapolate and then predict THC/11-OH-THC exposure after oral administration of THC, in special populations (e.g., maternal-fetal dyad, disease, genetic polymorphism), or in the presence of drug-drug interactions.

Acknowledgments

We would like to acknowledge the University of Washington (UW) Pharmacokinetics of Drug Abuse during Pregnancy team members for insightful discussion.

Authorship Contributions

Participated in research design: Patilea-Vrana, Unadkat.

Conducted experiments: Patilea-Vrana.

Contributed new reagents or analytic tools: Patilea-Vrana.

Performed data analysis: Patilea-Vrana.

Wrote or contributed to the writing of the manuscript: Patilea-Vrana, Unadkat.

References

Anderson GD (2005) Pregnancy-induced changes in pharmacokinetics: a mechanistic-based approach. *Clin Pharmacokinet* **44**:989–1008.

Anoshchenko O, Prasad B, Neradugomma NK, Wang J, Mao Q, and Unadkat JD (2020) Gestational age-dependent abundance of human placental transporters as determined by quantitative targeted proteomics. *Drug Metab Dispos* **48**:735–741.

Bailey JR, Cunny HC, Paule MG, and Slikker Jr W (1987) Fetal disposition of delta 9-tetrahydrocannabinol (THC) during late pregnancy in the rhesus monkey. *Toxicol Appl Pharmacol* **90**:315–321.

Barkus E, Morrison PD, Vuletic D, Dickson JC, Ell PJ, Pilowsky LS, Brenneisen R, Holt DW, Powell J, Kapur S, et al. (2011) Does intravenous Δ9-tetrahydrocannabinol increase dopamine release? A SPET study. *J Psychopharmacol* **25**:1462–1468.

Barnett G, Chiang CW, Perez-Reyes M, and Owens SM (1982) Kinetic study of smoking marijuana. *J Pharmacokinet Biopharm* **10**:495–506.

Blackard C and Tennes K (1984) Human placental transfer of cannabinoids. *N Engl J Med* **311**:797.

Bonhomme-Faivre L, Benyamina A, Reynaud M, Farinotti R, and Abbara C (2008) Disposition of Delta tetrahydrocannabinol in CF1 mice deficient in mdr1a P-glycoprotein. *Addict Biol* **13**:295–300.

Brockman AH, Oller HR, Moreau B, Kriksciukaite K, and Bilodeau MT (2015) Simple method provides resolution of albumin, lipoprotein, free fraction, and chylomicron to enhance the utility of protein binding assays. *J Med Chem* **58**:1420–1425.

Chandra S, Radwan MM, Majumdar CG, Church JC, Freeman TP, and ElSohly MA (2019) New trends in cannabis potency in USA and Europe during the last decade (2008-2017). *Eur Arch Psychiatry Clin Neurosci* **269**:5–15.

Desrosiers NA, Himes SK, Scheidweiler KB, Concheiro-Guisan M, Gorelick DA, and Huestis MA (2014) Phase I and II cannabinoid disposition in blood and plasma of occasional and frequent smokers following controlled smoked cannabis. *Clin Chem* **60**:631–643.

ElSohly MA, Ross SA, Mehmedic Z, Arafat R, Yi B, and Banahan 3rd BF (2000) Potency trends of delta9-THC and other cannabinoids in confiscated marijuana from 1980-1997. *J Forensic Sci* **45**:24–30.

Giroud C, Ménétrey A, Augsburger M, Buclin T, Sanchez-Mazas P, and Mangin P (2001) Delta(9)-THC, 11-OH-Delta(9)-THC and Delta(9)-THCCOOH plasma or serum to whole blood concentrations distribution ratios in blood samples taken from living and dead people. *Forensic Sci Int* **123**:159–164.

Grzeskowiak LE, Grieger JA, Andraweera P, Knight EJ, Leemaqz S, Poston L, McCowan L, Kenny L, Myers J, Walker JJ, et al. (2020) The deleterious effects of cannabis during pregnancy on neonatal outcomes. *Med J Aust* **212**:519–524.

Haddad S, Poulin P, and Krishnan K (2000) Relative lipid content as the sole mechanistic determinant of the adipose tissue:blood partition coefficients of highly lipophilic organic chemicals. *Chemosphere* **40**:839–843.

Han LW, Gao C, and Mao Q (2018) An update on expression and function of P-gp/ABCB1 and BCRP/ABCG2 in the placenta and fetus. *Expert Opin Drug Metab Toxicol* **14**:817–829.

Hebert MF, Easterling TR, Kirby B, Carr DB, Buchanan ML, Rutherford T, Thummel KE, Fishbein DP, and Unadkat JD (2008) Effects of pregnancy on CYP3A and P-glycoprotein activities as measured by disposition of midazolam and digoxin: a University of Washington specialized center of research study. *Clin Pharmacol Ther* **84**:248–253.

Huestis MA, Henningfield JE, and Cone EJ (1992) Blood cannabinoids. I. Absorption of THC and formation of 11-OH-THC and THCCOOH during and after smoking marijuana. *J Anal Toxicol* **16**:276–282.

Hunault CC, Böcker KB, Stellato RK, Kenemans JL, de Vries I, and Meulenbelt J (2014) Acute subjective effects after smoking joints containing up to 69 mg Δ9-tetrahydrocannabinol in recreational users: a randomized, crossover clinical trial. *Psychopharmacology (Berl)* **231**:4723–4733.

Hunault CC, Mensinga TT, de Vries I, Kelholt-Dijkman HH, Hoek J, Kruidenier M, Leenders ME, and Meulenbelt J (2008) Delta-9-tetrahydrocannabinol (THC) serum concentrations and pharmacological effects in males after smoking a combination of tobacco and cannabis containing up to 69 mg THC. *Psychopharmacology (Berl)* **201**:171–181.

Hunt CA and Jones RT (1980) Tolerance and disposition of tetrahydrocannabinol in man. *J Pharmacol Exp Ther* **215**:35–44.

Johansson E, Agurell S, Hollister LE, and Halldin MM (1988) Prolonged apparent half-life of delta 1-tetrahydrocannabinol in plasma of chronic marijuana users. *J Pharm Pharmacol* **40**:374–375.

Kauert GF, Ramaekers JG, Schneider E, Moeller MR, and Toennes SW (2007) Pharmacokinetic properties of delta9-tetrahydrocannabinol in serum and oral fluid. *J Anal Toxicol* **31**:288–293.

Ke AB, Nallani SC, Zhao P, Rostami-Hodjegan A, and Unadkat JD (2012) A PBPK model to predict disposition of CYP3A-metabolized drugs in pregnant women: verification and discerning the site of CYP3A induction. *CPT Pharmacometrics Syst Pharmacol* **1**:e3.

Ke AB, Nallani SC, Zhao P, Rostami-Hodjegan A, and Unadkat JD (2014) Expansion of a PBPK model to predict disposition in pregnant women of drugs cleared via multiple P450 enzymes, including CYP2B6, CYP2C9 and CYP2C19. *Br J Clin Pharmacol* **77**:554–570.

Kelly P and Jones RT (1992) Metabolism of tetrahydrocannabinol in frequent and infrequent marijuana users. *J Anal Toxicol* **16**:228–235.

Klausner HA, Wilcox HG, and Dingell JV (1975) The use of zonal ultracentrifugation in the investigation of the binding of delta9-tetrahydrocannabinol by plasma lipoproteins. *Drug Metab Dispos* **3**:314–319.

Lee D, Vandrey R, Mendu DR, Anizan S, Milman G, Murray JA, Barnes AJ, and Huestis MA (2013) Oral fluid cannabinoids in chronic cannabis smokers during oral δ9-tetrahydrocannabinol therapy and smoked cannabis challenge. *Clin Chem* **59**:1770–1779.

Lemberger L, Crabtree RE, and Rowe HM (1972a) 11-hydroxy- 9 -tetrahydrocannabinol: pharmacology, disposition, and metabolism of a major metabolite of marihuana in man. *Science* **177**:62–64.

Lemberger L, Martz R, Rodda B, Forney R, and Rowe H (1973) Comparative pharmacology of Delta9-tetrahydrocannabinol and its metabolite, 11-OH-Delta9-tetrahydrocannabinol. *J Clin Invest* **52**:2411–2417.

Lemberger L, Silberstein SD, Axelrod J, and Kopin IJ (1970) Marihuana: studies on the disposition and metabolism of delta-9-tetrahydrocannabinol in man. *Science* **170**:1320–1322.

Lemberger L, Tamarkin NR, Axelrod J, and Kopin IJ (1971) Delta-9-tetrahydrocannabinol: metabolism and disposition in long-term marihuana smokers. *Science* **173**:72–74.

Lemberger L, Weiss JL, Watanabe AM, Galanter IM, Wyatt RJ, and Cardon PV (1972b) Delta-9-tetrahydrocannabinol. Temporal correlation of the psychologic effects and blood levels after various routes of administration. *N Engl J Med* **286**:685–688.

Lindgren JE, Ohlsson A, Agurell S, Hollister L, and Gillespie H (1981) Clinical effects and plasma levels of delta 9-tetrahydrocannabinol (delta 9-THC) in heavy and light users of cannabis. *Psychopharmacology (Berl)* **74**:208–212.

Mariani JJ, Brooks D, Haney M, and Levin FR (2011) Quantification and comparison of marijuana smoking practices: blunts, joints, and pipes. *Drug Alcohol Depend* **113**:249–251.

McBurney LJ, Bobbie BA, and Sepp LA (1986) GC/MS and EMIT analyses for delta 9-tetrahydrocannabinol metabolites in plasma and urine of human subjects. *J Anal Toxicol* **10**:56–64.

McClure EA, Stitzer ML, and Vandrey R (2012) Characterizing smoking topography of cannabis in heavy users. *Psychopharmacology (Berl)* **220**:309–318.

Methaneethorn J, Poomsaidorn C, Naosang K, Kaewworasut P, and Lohitnavy M (2020) A Δ^9-tetrahydrocannabinol physiologically-based pharmacokinetic model development in humans. *Eur J Drug Metab Pharmacokinet* **45**:495–511.

Morrison PD, Zois V, McKeown DA, Lee TD, Holt DW, Powell JF, Kapur S, and Murray RM (2009) The acute effects of synthetic intravenous Delta9-tetrahydrocannabinol on psychosis, mood and cognitive functioning. *Psychol Med* **39**:1607–1616.

Naef M, Russmann S, Petersen-Felix S, and Brenneisen R (2004) Development and pharmacokinetic characterization of pulmonal and intravenous delta-9-tetrahydrocannabinol (THC) in humans. *J Pharm Sci* **93**:1176–1184.

Newmeyer MN, Swortwood MJ, Taylor ME, Abulseoud OA, Woodward TH, and Huestis MA (2017) Evaluation of divided attention psychophysical task performance and effects on pupil sizes following smoked, vaporized and oral cannabis administration. *J Appl Toxicol* **37**:922–932.

O'Sullivan MJ, Boyer PJ, Scott GB, Parks WP, Weller S, Blum MR, Balsley J, and Bryson YJ; Zidovudine Collaborative Working Group (1993) The pharmacokinetics and safety of zidovudine in the third trimester of pregnancy for women infected with human immunodeficiency virus and

their infants: phase I acquired immunodeficiency syndrome clinical trials group study (protocol 082). *Am J Obstet Gynecol* **168**:1510–1516.

Ohlsson A, Lindgren JE, Wahlen A, Agurell S, Hollister LE, and Gillespie HK (1980) Plasma delta-9 tetrahydrocannabinol concentrations and clinical effects after oral and intravenous administration and smoking. *Clin Pharmacol Ther* **28**:409–416.

Ohlsson A, Lindgren JE, Wahlén A, Agurell S, Hollister LE, and Gillespie HK (1982) Single dose kinetics of deuterium labelled delta 1-tetrahydrocannabinol in heavy and light cannabis users. *Biomed Mass Spectrom* **9**:6–10.

Pang KS, Morris ME, and Sun H (2008) Formed and preformed metabolites: facts and comparisons. *J Pharm Pharmacol* **60**:1247–1275.

Patilea-Vrana GI, Anoshchenko O, and Unadkat JD (2018) Hepatic enzymes relevant to the disposition of (-)-Δ^9-tetrahydrocannabinol (THC) and its psychoactive metabolite, 11-OH-THC. *Drug Metab Dispos* **47**:249–256.

Patilea-Vrana GI and Unadkat JD (2019) Quantifying hepatic enzyme kinetics of (-)-Δ^9-tetrahydrocannabinol (THC) and its psychoactive metabolite, 11-OH-THC, through in vitro modeling. *Drug Metab Dispos* **47**:743–752.

Perez-Reyes M, Di Guiseppi S, Davis KH, Schindler VH, and Cook CE (1982) Comparison of effects of marihuana cigarettes to three different potencies. *Clin Pharmacol Ther* **31**:617–624.

Rodgers T and Rowland M (2007) Mechanistic approaches to volume of distribution predictions: understanding the processes. *Pharm Res* **24**:918–933.

SAMHSA (2018) *Key Substance Use and Mental Health Indicators in the United States: Results from the 2018 National Survey on Drug Use and Health*, Substance Abuse and Mental Health Services Administration, Rockville, MD.

Schauer GL, King BA, Bunnell RE, Promoff G, and McAfee TA (2016) Toking, vaping, and eating for health or fun: marijuana use patterns in adults, U.S., 2014. *Am J Prev Med* **50**:1–8.

Schwilke EW, Karschner EL, Lowe RH, Gordon AM, Cadet JL, Herning RI, and Huestis MA (2009) Intra- and intersubject whole blood/plasma cannabinoid ratios determined by 2-dimensional, electron impact GC-MS with cryofocusing. *Clin Chem* **55**:1188–1195.

Schwope DM, Karschner EL, Gorelick DA, and Huestis MA (2011) Identification of recent cannabis use: whole-blood and plasma free and glucuronidated cannabinoid pharmacokinetics following controlled smoked cannabis administration. *Clin Chem* **57**:1406–1414.

Sheiner LB and Beal SL (1981) Some suggestions for measuring predictive performance. *J Pharmacokinet Biopharm* **9**:503–512.

Spiro AS, Wong A, Boucher AA, and Arnold JC (2012) Enhanced brain disposition and effects of Δ9-tetrahydrocannabinol in P-glycoprotein and breast cancer resistance protein knockout mice. *PLoS One* **7**:e35937.

Stickrath E (2019) Marijuana use in pregnancy: an updated look at marijuana use and its impact on pregnancy. *Clin Obstet Gynecol* **62**:185–190.

Tasnif Y, Morado J, and Hebert MF (2016) Pregnancy-related pharmacokinetic changes. *Clin Pharmacol Ther* **100**:53–62.

Thomas BF, Compton DR, and Martin BR (1990) Characterization of the lipophilicity of natural and synthetic analogs of delta 9-tetrahydrocannabinol and its relationship to pharmacological potency. *J Pharmacol Exp Ther* **255**:624–630.

Toennes SW, Ramaekers JG, Theunissen EL, Moeller MR, and Kauert GF (2008) Comparison of cannabinoid pharmacokinetic properties in occasional and heavy users smoking a marijuana or placebo joint. *J Anal Toxicol* **32**:470–477.

Toennes SW, Schneider K, Kauert GF, Wunder C, Moeller MR, Theunissen EL, and Ramaekers JG (2011) Influence of ethanol on cannabinoid pharmacokinetic parameters in chronic users. *Anal Bioanal Chem* **400**:145–152.

Wall ME, Brine DR, Pitt CG, and Perez-Reyes M (1972) Identification of 9 -tetrahydrocannabinol and metabolites in man. *J Am Chem Soc* **94**:8579–8581.

Wall ME and Perez-Reyes M (1981) The metabolism of delta 9-tetrahydrocannabinol and related cannabinoids in man. *J Clin Pharmacol* **21** (S1):178S–189S.

Wall ME, Sadler BM, Brine D, Taylor H, and Perez-Reyes M (1983) Metabolism, disposition, and kinetics of delta-9-tetrahydrocannabinol in men and women. *Clin Pharmacol Ther* **34**:352–363.

Wolowich WR, Greif R, Kleine-Brueggeney M, Bernhard W, and Theiler L (2019) Minimal physiologically based pharmacokinetic model of intravenously and orally administered delta-9-tetrahydrocannabinol in healthy volunteers. *Eur J Drug Metab Pharmacokinet* **44**:691–711.

Zhang Z, Farooq M, Prasad B, Grepper S, and Unadkat JD (2015) Prediction of gestational age-dependent induction of in vivo hepatic CYP3A activity based on HepaRG cells and human hepatocytes. *Drug Metab Dispos* **43**:836–842.

Zhang Z, Imperial MZ, Patilea-Vrana GI, Wedagedera J, Gaohua L, and Unadkat JD (2017) Development of a novel maternal-fetal physiologically based pharmacokinetic model I: insights into factors that determine fetal drug exposure through simulations and sensitivity analyses. *Drug Metab Dispos* **45**:920–938.

Zhang Z and Unadkat JD (2017) Development of a novel maternal-fetal physiologically based pharmacokinetic model II: verification of the model for passive placental permeability drugs. *Drug Metab Dispos* **45**:939–946.

Address correspondence to: Dr. Jashvant D. Unadkat, Department of Pharmaceutics, University of Washington, Box 357610, Seattle, WA 98195. E-mail: jash@uw.edu